Journal of Materials Chemistry B

Accepted Manuscript

This is an *Accepted Manuscript*, which has been through the Royal Society of Chemistry peer review process and has been accepted for publication.

Accepted Manuscripts are published online shortly after acceptance, before technical editing, formatting and proof reading. Using this free service, authors can make their results available to the community, in citable form, before we publish the edited article. We will replace this *Accepted Manuscript* with the edited and formatted *Advance Article* as soon as it is available.

You can find more information about *Accepted Manuscripts* in the Information for Authors.

Please note that technical editing may introduce minor changes to the text and/or graphics, which may alter content. The journal's standard Terms & Conditions and the Ethical guidelines still apply. In no event shall the Royal Society of Chemistry be held responsible for any errors or omissions in this *Accepted Manuscript* or any consequences arising from the use of any information it contains.

ROYAL SOCIETY OF CHEMISTRY

www.rsc.org/materialsB

Journal of Materials Chemistry B RSCPublishing

ARTICLE

Incorporating Fluorescent Dyes into Monodisperse Melamine-Formaldehyde Resin Microspheres via Organic Sol-Gel Process: Pre-polymer Doping Strategy

Cite this: DOI: 10.1039/x0xx00000x

Received 00th January 2012,
Accepted 00th January 2012

DOI: 10.1039/x0xx00000x

www.rsc.org/

Youshen Wu[a], Yan Li[a], Jianhua Xu[b] and Daocheng Wu[a]

An organic sol-gel process was developed to incorporate fluorescent dyes into monodisperse melamine-formaldehyde (MF) resin microspheres. Various organic fluorescent dyes have been successfully incorporated by this process, and monodisperse fluorescent MF microspheres were prepared. Fluorescence-encoded microsphere arrays with dozens of sets were obtained by quantitatively incorporating several dyes at different doping concentrations. The characteristics and incorporating mechanism of these microspheres and their dyes were investigated by scanning electron microscopy, Malvern particle analysis, fluorescence spectroscopy, laser scanning confocal microscopy (LSCM), and flow cytometric analyses. Resonance energy transfer (RET) interactions of the doped dyes were investigated by steady-state and time-resolved fluorescence spectroscopy. The dye-incorporated microspheres were stable, and no leakage or deformation was found. With the occurrence of the RET effect among multi-doped dyes, prepared microspheres exhibited a single excited, doping ratio-related emission signatures. The prepared dye-doped microspheres were coated with silica shells, which provided favorable surface properties for bioconjugate applications. This process of incorporating organic dye could also be used to coat particles with dye-doped fluorescent MF shells. Multi-shell structured composite microspheres with fluorescent shells were also prepared by alternately repeating silica and MF coatings.

1. Introduction

As fluorescent markers, assay substrates, and instrument standards, fluorescent microspheres have been used in applications such as *in vivo* imaging,[1] cell labelling,[2, 3] fluorescence sensing,[4-8] random laser,[9, 10] and colloidal assembly.[11-13] In particular, microsphere arrays with sets of fluorescence-encoded microspheres (exhibiting different fluorescence emission signatures) can be used as suspension arrays for powerful, flexible, and high-throughput multiplex assays. Since the pioneering work of Nie et al. in 2001, studies in this area have drawn much attention.[14-18]

Fluorescent microspheres are prepared by binding fluorophores [e.g., organic fluorescent dyes,[4, 7, 12, 14, 19-23] metal-ligand complexes,[8, 24] quantum dots (QDs),[1, 25, 26] rare-earth upconversion nanoparticles (NPs),[27] and conjugated polymers[28, 29]] with microsphere substrates [e.g., polystyrene (PS),[14, 22, 23, 26, 30] polymethylmethacrylate,[12, 31] SiO_2[1, 25, 28] and TiO_2[32]] in certain physical/chemical processes. Fluorophores have been incorporated or doped into the interior or tagged on the surface of the microspheres by non-covalent (absorption[21, 22, 31] and physical trapping[17, 20, 23, 25, 26]) or covalent (co-polymerization[33] and conjugation[19, 22, 34]) binding processes. Compared with common fluorescent microspheres, fluorescence-encoded microspheres have multifaceted nature and have very high demand; as encoded microcarriers, these microspheres should be monodisperse, have quantitative emissions in one or more wavelengths, and have modifiable surfaces for bioconjugation.[15, 16, 23]

QDs and organic fluorescent dyes are typically used in preparing fluorescence-encoded microspheres.[15, 16, 18] QDs are semiconductor NPs that exhibit bright, stable, and turnable fluorescent emissions,[17] which are ideal fluorescent tags for preparing fluorescence-encoded microspheres. However, considering the colloidal nature of the QD NPs, incorporating these particles involves the use of complex multi-step processes or special equipment.[17, 25, 26, 35] Fluorescent dyes are easier to handle and of better batch uniformity than NP fluorophores, which are conducive for fabricating microsphere arrays with large number of encoded carriers in practice.

Commercially available fluorescence-encoded microspheres were prepared by doping one or two dyes into the PS microspheres in solvent-swelling processes.[15, 16, 18] In such processes, microspheres were swelled in organic solution that contains one or two dyes, allowing the dyes to diffuse in and be transferred to aqueous solution. The swelled microspheres shrink in aqueous solution with entrapped dyes.[15] Besides solvent swelling, several attempts were also proposed by

Journal of Materials Chemistry B Accepted Manuscript

researchers. Martin-Banderas reported their preparation of fluorescence-encoded microspheres in combination with flow-focusing technology and solvent extraction/evaporation processes.[14] Through these processes, four types of dyes could be incorporated into sets of fluorescent microspheres quantitatively, and several sets of products were prepared. Zhang et al. reported their preparation of fluorescence-encoded microspheres in a core-shell structure.[23] Rhodamine 6G was quantitatively incorporated into the cross-linked polymer shell of the microspheres, 12 sets of microspheres that exhibit different emission intensities were prepared. However, these methods are usually suitable only for incorporating some specific dyes; the number of simultaneously doped dyes is usually less than two; furthermore, doping mechanisms are seldom reported.

Given the physical nature of organic dyes and current developed processes, some difficulties still exist to simultaneously incorporate multiple dyes into the microsphere substrate: 1) Dyes of different solubilities are difficult to simultaneously incorporate with similar efficiency;[23, 36, 37] 2) As aggregation of dye molecules will lead to red-shift and drastic decrease in fluorescence emissions, uneven distribution of the dyes in the substrate may lead to changes in fluorescence properties;[36, 38, 39] 3) If multiple dyes with overlapped emission and excitation spectra are simultaneously doped, radiative and/or non-radiative energy transfer may complicate the code.[7, 15, 33, 40, 41] Therefore, novel processes with wider dye adaptability, higher incorporation precision, and controllable dye distribution are highly demanded.

In our previous work, we have developed an organic sol-gel process that is rapid, effective, and surfactant-free for preparing monodisperse melamine-formaldehyde (MF) resin microspheres.[42] The prepared microspheres are highly monodisperse with controllable size of 0.5 μm to 8.0 μm. They have highly cross-linked and porous interior structure,[43] showing high tolerance to organic solvents and good thermal stability. MF microspheres are prepared with MF pre-polymer in an organic sol-gel process. If fluorescent dyes were initially dissolved in a solvent, such as dimethylsulfoxide (DMSO), and further mixed with MF pre-polymer solution, these dyes could be doped with the branched MF pre-polymers and be incorporated within the microsphere substrate during the organic sol-gel particle formation process.

With investigation of the dye-doping mechanism of the organic sol-gel process of MF, we developed a simple and facile method for preparing fluorescence-encoded MF microspheres. Fluorescence-encoded microspheres with different encoding schemes were successfully prepared. Miscellaneous dyes were dissolved in DMSO and doped with pre-polymer solution via pre-polymer doping strategy, and were then incorporated into the formed monodisperse MF microspheres. Dye encapsulation efficiencies are higher than 99% even at high doping concentrations of 20 $\mu mol \cdot g^{-1}$. Multiple dyes with different solubilities could be simultaneously and quantitatively doped, the emission signature of the products could be finely adjusted by changing the doping ratio of the doped dyes. Microsphere arrays containing 25 fluorescence-encoded emissions have been prepared by using two dyes with five different concentrations each. Microsphere arrays containing 27 fluorescence-encoded emissions have been prepared by using three dyes with three different concentrations each. This organic sol-gel process could also be applied to coat particles with layers of fluorescence-encoded shells. We have prepared $(MF@silica)_2$ $[(M@S)_2]$ and $(MF@silica)_3$ $[(M@S)_3]$ composite particles to demonstrate the effectiveness and agility of this method by coating the pre-prepared MF@silica (M@S) core-shell microspheres with one and two layers of fluorescent shells (with thin silica shell between the MF shells).

2. Results and Discussion

2.1. Dye incorporating process and doping mechanism

Macromolecules with branched molecular structures, such as dendrimers and dendrons, have been used to incorporate small molecules including drugs and dyes.[44, 45] MF pre-polymers are branched water-soluble polymers, under heating and acid catalysis, which could further polymerize into MF NPs and grow into MF microspheres upon further aggregation. To investigate the interaction of the dye molecule with the MF pre-polymer, 8-anilino-1-naphthalenesulfonic acid (ANS) was used as model dye for the doping process. As a fluorescent polarity probe, ANS has been used for investigating the local structure and dynamics in sol-gel derived nanocomposite materials.[46, 47] ANS has polarity-related emission characteristics, in which emission intensities and maximum emission wavelengths could change in surroundings of different polarities.[48] ANS dyes were initially dissolved with DMSO, and the DMSO solution of ANS was mixed with pre-prepared MF pre-polymer solution to allow the ANS dye molecules to dope into the pre-polymer molecules.

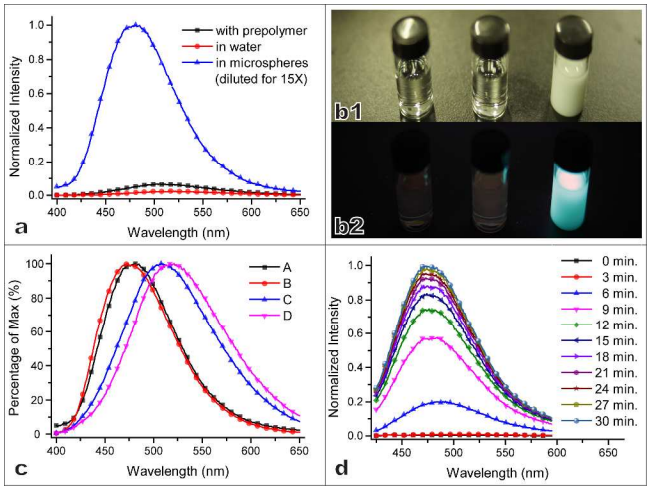

Figure 1. (a) Emission intensity comparison for the ANS dyes in different media. From top to bottom: ANS incorporated within the MF microspheres; ANS bounded with MF pre-polymer and ANS in water, with excitation of 380nm. (b1-b2) From left to right: ANS solution; mixture of ANS solution and MF pre-polymer solution and prepared ANS doped MF microspheres with normal and UV illumination. (c) Maximum emission wavelength comparison for ANS dyes in different media: (from A to D) in MF microspheres, in DMSO, with MF pre-polymer and in water, with excitation of 380nm. (d) From bottom to top: emission spectra of the reaction system during the organic sol-gel process in 0 to 30 minutes, with excitation of 380nm.

The fluorescence intensity of the mixture of ANS and MF pre-polymer was enhanced for about 2.7 times compared with that water of ANS, and the maximum emission intensity of the dye-pre-polymer mixture was blue-shifted by 12 nm (from 520 nm to 508 nm) than that of the ANS water solution. These changes in fluorescence emission showed the association of ANS and MF pre-polymer molecules, which is also observed in the mixture of ANS and protein solution.[49] While the solution of MF pre-polymer and ANS dye were heated at 100 °C (boiling

Journal of Materials Chemistry B Accepted Manuscript

This journal is © The Royal Society of Chemistry 2012

bath), inter- and intro-molecular cross-linking occurred in between the dye-doped MF pre-polymer molecules, and the emission spectra of the ANS dye further changed during the process. The emission intensity of the system increased by 255 times after the sol-gel process, while its maximum emission wavelength blue-shifted from 508 nm to 480 nm. These changes indicated that the ANS dye molecules have been incorporated into the formed MF microspheres, as the polarity of their local surrounding significantly decreased. By observing under a fluorescence microscope, we determined that the prepared dye-incorporated products are monodisperse microspheres that exhibit blue fluorescence emission under ultraviolet excitation of 365 nm (Figure 1 a to c and Figure S1 a2).

In situ measurement of the emission spectra of the reaction system recorded the time-dependent fluorescence emission changes of the doped ANS dye molecules during the organic sol-gel process of the MF. These time-dependent emission spectra reflected the changes in polarity of the dye's local surrounding during the reaction, thereby profiling the dynamics of the organic sol-gel process. Figure 1 d shows the fluorescence emission spectra of the reaction system (every 3 min since reaction began) during the organic sol-gel process (original data were recorded every 30 s, and complete spectra are shown in Figure S2 and S3). During the organic sol-gel process, the fluorescence emission characteristics of the ANS probe gradually changed. Fluorescence emission was relatively stable in the first 3 min, sharply increased during the next 18 min, and stabilized in the last 9 min (Figure S4). The maximum emission wavelength also gradually blue-shifted as the emission intensity increased (Figure S5).

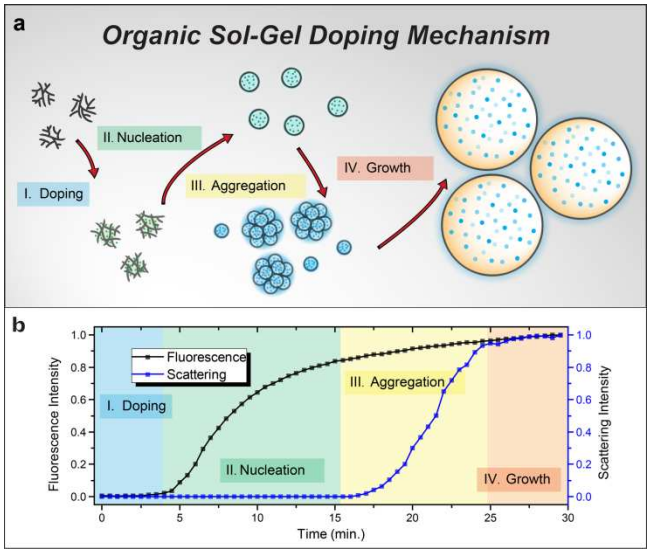

Figure 2. (a) Schematic illustration of the four-stage organic sol-gel doping mechanism. (b) Fluorescence emission intensity (of ANS) and scattering intensity monitoring of the complete organic sol-gel process.

The scattering intensity of the system also changed during the process (Figure 2 b). However, the changes in fluorescence occurred earlier than that of scattering. Changes in scattering and fluorescence emission intensities originated from different physical events. As previously reported[42], the changes in scattering intensity indicated the formation of MF NPs, which was confirmed by time-resolved transmission electron microscopy analysis.[42] Changes in fluorescence emission indicated that the ANS probe molecules were incorporated into some local surroundings that preserve less polarity than water. Therefore, the difference in changes of scattering and fluorescence emission intensities during the process may be ascribed to the following dye-doping mechanisms: 1) Probe dye molecules were initially associated with the branched MF pre-polymer molecules, exhibiting an emission that is different from pure water; 2) These molecules were further wrapped with polymer, whereas the pre-polymer molecules were cross-linked, leading to gradual changes in fluorescence emission; 3) The dye-doped pre-polymer molecules were further cross-linked, forming MF NPs, which resulted in sharp increase in scattering and further changes in fluorescence emission; and 4) The formed MF NPs aggregated with each other and eventually grew into MF microspheres, with dye molecules doped in. Figure 2 a shows these four stages, i.e., doping, nucleation, aggregation, and growth.

2.2. Fluorescence-encoded micro carriers with single dye doped microspheres

Further experiments showed that the dye-incorporating process is valid for various dyes other than ANS. Organic fluorescent dyes, including Acridine (Acr), Acridine Orange (AO), Rhodamine 110 (Rh 110), Rhodamine B (Rh B), Sulforhodamine 101 (SRh 101), 7-amino-4-methylcoumarin (AMC), Nile Blue (NB), and fluorescein (Flu) could all be incorporated into the monodisperse MF microspheres with similar pre-polymer doping strategy. Addition of dyes took little influence to the morphology of the product. With initial pre-polymer concentrations of 13, 25, 38, 50, 63, and 76 $mg \cdot mL^{-1}$, monodisperse dye-doped microspheres with controllable average diameters of 1.72, 2.71, 3.35, 4.62, 5.89, and 6.81 μm (with CV values of 3.4%, 2.7%, 2.6%, 3.1%, 3.3% and 3.3%) were prepared (Figure 3). The prepared microspheres exhibit fluorescence emissions that correspond to the doped dyes under ultraviolet excitation of 365 nm. (Figure 4 a and b, Figure S1)

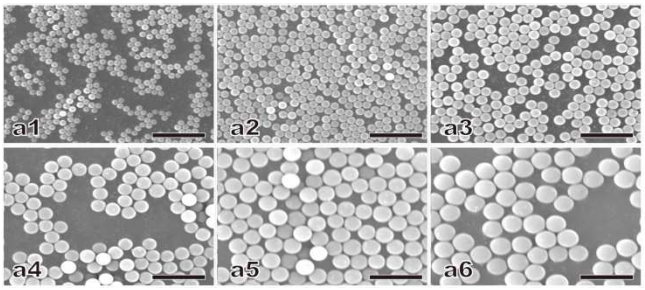

Figure 3. SEM images of prepared dye-doped MF microspheres of different sizes. From a1 to a6: microspheres with average diameters of 1.72, 2.71, 3.35, 4.62, 5.89 and 6.81μm. Scale bars=10 μm.

For most of the used dyes, the dye-doped microsphere samples exhibit red-shifted maximum emission wavelengths compared with that of the water solution of the dyes. (Figure S6) Dye encapsulation rate obtained by the organic sol-gel process is very high. Dyes of different solubilities, such as Rh 110, Rh B, and SRh 101, could all be incorporated into the formed MF microspheres in encapsulation rates that are higher than 99%. By using an initial pre-polymer concentration of 30 $mg \cdot mL^{-1}$ and dye addition of 20, 60, 180, and 540 nmol, and 1.62 and 4.96 μmol, microspheres with corresponding doping concentrations of 35, 105, 320, and 960 $nmol \cdot g^{-1}$, and 2.9 and 8.7 $\mu mol \cdot g^{-1}$ were prepared by this process (Figure 4 b).

Journal of Materials Chemistry B Accepted Manuscript

Quantitative measurements revealed that microsphere samples exhibit quantitative fluorescence emission intensities that are associated with the initial dye additions and present linear relationship over a wide range (Figure 4 c).

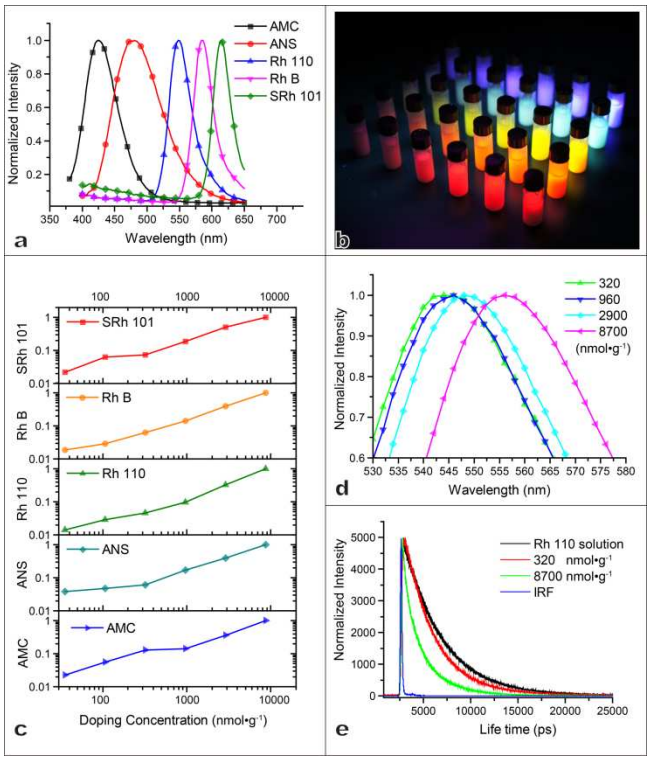

Figure 4. (a) From left to right: normalized emission spectra of MF microspheres doped with AMC, ANS, Rh 110, Rh B and SRh 101 dyes. (b) MF microsphere samples doped with AMC (bluish violet), ANS (blue), Rh 110 (yellow), Rh B (orange) and SRh 101 dye (red) in 6 concentrations under UV illumination. (c) From top to bottom: fluorescence emission intensity versus doping concentration curves of SRh 101, Rh B, Rh 110, ANS and AMC dyes doped samples, excited at 360nm for AMC doped samples and excited at 380nm for other 4 dyes doped samples. (d) Normalized emission spectra of Rh 110 dye doped MF microspheres with increased doping concentrations, with increasing doping concentration, the emission peaks shifted to longer wavelengths, excited at 380nm. (e) Fluorescence lifetime decay curves of Rh 110 dye in solution and Rh 110 dye doped in MF microspheres with different doping concentrations.

The prepared microsphere samples with high dye additions also possess a doping concentration-related red-shift in maximum emission wavelengths (Figure 4 d and Figure S7).

Time-resolved fluorescence spectra of the samples with different doping concentrations were measured to validate the effect of homo RET, and fluorescence lifetimes were calculated (Figure 4 e). The calculated fluorescence lifetime of the Rh 110 solution is 3.79 ns, whereas those of the Rh 110-doped microsphere samples are 2.97 ns (with doping concentration of 320 nmol·g^{-1}) and 2.10 ns (with doping concentration of 8.7 μmol·g^{-1}). As the fluorescence decay rate of the dyes changed in medium of different polarizabilities,[50] the shorter lifetime of the dye-doped microspheres than that of the dye solution could be attributed to the different polarizability of the MF microsphere substrate (compared with water). However, decrease in the fluorescence lifetime of samples with high doping concentrations may result from the homo RET effect. At doping concentration of 8.79 μmol·g^{-1}, the average distance of the doped dyes is about 4 nm (see Supporting Information for calculation), which is in the distance range of homo RET (3 nm to 4 nm for common dyes[51, 52]). Though homo RET was proved in samples with higher doping concentrations, emission intensities of these samples are still higher than those samples with lower doping concentrations; little quench was observed even for samples with doping concentration higher than 10 μmol·g^{-1}, which indicating an evenly distribution of the dye molecules in the substrate of the MF microspheres, as combined aggregation and homo RET would lead to drastic self-quenching of the dyes.[53]

To investigate the possibility of using dye-doped MF microspheres as microcarriers, microsphere samples that were doped with different doping concentrations were analyzed using a flow cytometer (Figure S9 a1–6). The results showed that the prepared microspheres exhibit narrowly distributed fluorescence emission, indicating their monodisperse size. Samples with different doping concentrations exhibit different fluorescence emission intensities. LSCM analysis of the samples also confirmed that the prepared microspheres are uniform in both size and fluorescence emission.

To facilitate the bioconjugation application of the prepared MF fluorescent microspheres, silica coating was performed, and fluorescent MF@silica core-shell microspheres (M@S) were prepared. Given the high stability of the MF in organic solvents, the silica coating process did not lead to any breakage or leakage to the fluorescent MF microspheres, and the prepared M@S exhibited fluorescence properties that are similar to those of uncoated ones. These findings indicated their availability as encoded microcarriers for multiplexed assays.

By using five dyes with five different doping concentrations each, we prepared 25 sets of fluorescent microspheres, which are encoded by the corresponding 25 different emissions signatures (Figure 4 b).

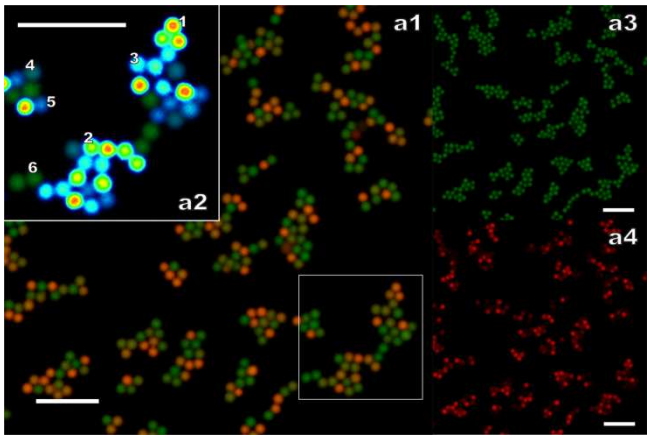

Figure 5. (a1) LSCM image of mixture of six sets of M@S microspheres doped with 2 dyes (Rh 110 and SRh 101) in 6 different ratios under 488nm excitation. (a2) A Part of the digital enhanced image, with six distinguishable microsphere sets noted. (a3-a4) Two separated channels (Rh 110 and SRh 101) of the image. Scale bars=10 μm.

2.3. Preparation of multi-doped fluorescence-encoded microspheres

The encoding capacity of the fluorescence-encoded microcarriers could be amplified using multiple dyes. As pointed out in the literature,[15, 16, 18] if N dyes and M doping concentrations are used for the encoding signatures, the potential encoding capacity (C) is C = M^N. Evidently, simultaneous doping of multiple dyes into the microspheres could be an effective method for fabricating larger microsphere

Journal of Materials Chemistry B Accepted Manuscript

This journal is © The Royal Society of Chemistry 2012

arrays. It was found, multiple dyes with different physical properties (solubility and fluorescence) could be simultaneously incorporated into the monodisperse MF microspheres in this organic sol-gel process. The prepared products are monodisperse. In addition, microsphere batches that were prepared with different dye additions (added with dyes of different ratios and total amounts) shared similar average sizes (which could be related with the initial pre-polymer concentration only) and exhibited distinct fluorescence emissions under similar excitation. Figure 5 a1 shows the LSCM image of the mixture of six sets of M@S microspheres that were doped with two dyes (Rh 110 and SRh 101) in six different ratios. Figure 5 a2 shows part of the digital enhanced image, in which six microsphere sets are distinguishable. Figure S9 b1 and 2 shows the fluorescence profile resulting from the analysis of the mixture of these dual-doped samples in a flow cytometer, in which six sets could be well distinguished. Triple-doped samples were also obtained by this process. Figure 6 d shows the emission spectra of microsphere samples that were doped with one (Rh 110), two (Rh 110 and SRh 101), and three dyes (Rh 110, SRh 101, and NB).

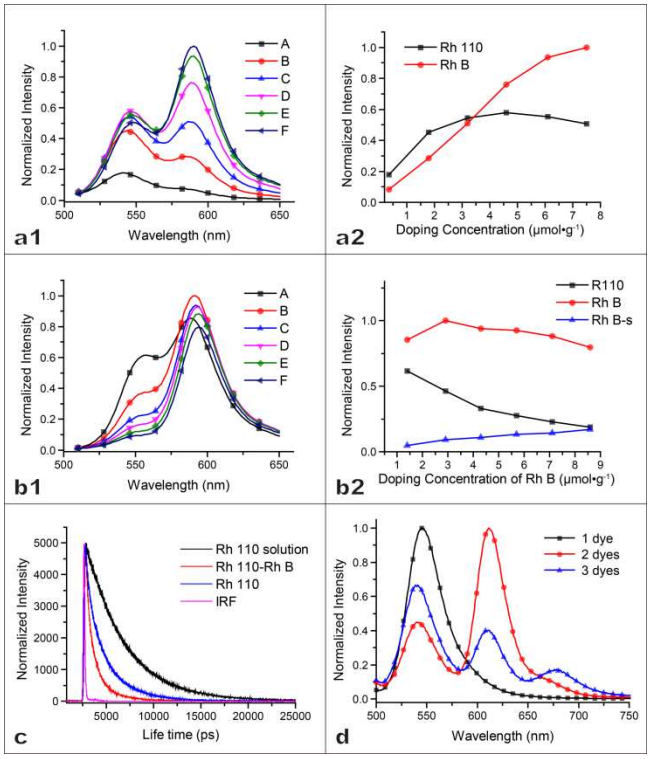

Figure 6. (a1) Emission spectra of MF microspheres doped with Rh 110 and Rh B dyes in different total concentrations. The total doping concentrations are: (from A to F) 0.36, 1.8, 3.2, 4.6, 6.1 and 7.5μmol·g^{-1}), excited at 488nm. (a2) Emission intensity versus doping concentration curves of the doped dyes. (b1) Emission spectra of MF resin microspheres doped with constant Rh 110 concentration and increased Rh B dyes concentrations, excited at 488nm. The molar ratios of doped Rh 110: Rh B dyes are: (from A to F) 6:1, 6:2, 6:3, 6:4, 6:5 and 6:6. (b2) Curve Rh 110 and Rh B are emission intensity versus Rh B doping concentration curves of the doped dyes in the dual doped microspheres. Curve Rh B-s is the emission intensity versus Rh B doping concentration curve of samples doped with only Rh B dye and excited at same excitation wavelength (488nm). (c) Fluorescence lifetime decay curves of Rh 110 dye in solution, doped in MF microspheres and simultaneously doped with Rh B. (d) Emission spectra of MF resin microspheres doped with one (Rh 110), two (Rh 110 and SRh 101) and three dyes (Rh 110, SRh 101 and NB).

As previously mentioned, if multiple dyes with overlapped spectra are simultaneously doped, the radiative and/or non-radiative energy transfer might complicate the emission signature. The RET process among the doped multiple dyes may exhibit nova fluorescence properties in prepared materials.[32, 33, 41, 52, 53] Silica NPs that were doped with three dyes with tandem excitation and emission spectra exhibit unique single excited multi-emission properties, which were used for multiplexed assays.[40, 54] RET effects of the doped dyes were also used for functional materials for applications such as pH sensor random laser.[7, 10]

Given that RET is a process that is strongly influenced by the distance of the donor and the acceptor dyes, the total doping concentration (average distance of the doped dyes) will affect the obtained emission signature. To investigate the influence of total doping concentration, a pair of dyes, namely, Rh 110 (acts as a donor in the RET process) and Rh B (acts as an acceptor), was doped in increasing total doping concentrations (from 0.36, 1.8, 3.2, 4.6, and 6.1 μmol·g^{-1} to 7.5 μmol·g^{-1}) and constant mole ratio of 1:1. Figure 6 a1 shows the emission spectra of the prepared samples. Figure 6 a2 shows the emission intensity versus total doping concentration curves of the Rh 110 and Rh B dyes. With increased total doping concentrations, the acceptor dye's emission intensity increased, whereas the donor dye emission intensity dropped after the first growth. With increased total doping concentration, the average inter-distance of the doped dyes decreased, and the RET effect of the donor and acceptor dyes became more significant.

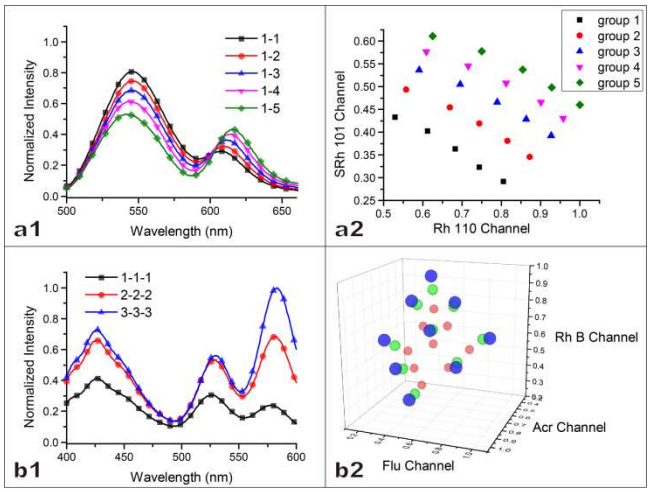

Figure 7. (a1) Representative emission spectra of dual-encoded (Rh 110 and SRh 101) MF microspheres. (a2) Emission intensity distribution of 25 sets of the dual-encoded (Rh 110 and SRh 101) MF microspheres. Axes scales are emission intensity at wavelength of 545nm (for Rh 110 channel) and 612nm (for SRh 101 channel). (b1) Representatives emission spectra of triple-encoded (Acr, Flu and Rh B) MF micro-spheres. (b2) Emission intensity distribution of 27 sets of the triple encoded (Acr, Flu and Rh B) MF microspheres. Axes scales are emission intensity at wavelength of 426nm (for Acr channel), 528nm (for Flu channel) and 582nm (for Rh B channel)

Figure 6 c shows the fluorescence decay curves of the Rh 110 solution (5 μmol·L^{-1}), Rh 110-doped microspheres at doping concentration of 8.79 μmol·g^{-1}, and Rh 110 and Rh B dual-doped microsphere samples with high total doping concentration of 7.5 μmol·g^{-1}. The fluorescence lifetime of the dual-doped microsphere samples (1.06 ns) is shorter than that of the dye solution (3.79ns) and those of the single-doped microsphere samples (2.10ns), indicating high RET efficiency between the dual-doped dyes.[7, 52]

Journal of Materials Chemistry B Accepted Manuscript

To investigate the influence of mole ratio of the doped dyes to the RET processes, Rh 110 and Rh B, was doped with constant donor concentration (8.6 μmol·g^{-1}) and varied donor: acceptor ratios of 6:1, 6:2, 6:3, 6:4, 6:5, and 6:6. Figure 6 b1 shows the emission spectra of the prepared samples. With increased acceptor doping concentrations, the donor dye emission intensity decreased. The acceptor dye emission intensity dropped after the first growth, though its own doping concentration increased. It was also found that with the presence of the donor dye, the doped acceptor dyes exhibit brighter emissions than their single-doped counterparts under the same excitation wavelength (Figure. 6 b2). This enhanced emission could be attributed to the "antenna effect" of the donor dyes, in which multiple excited donor dyes could transfer their energy to one acceptor dye, thus providing the acceptor dye with enhanced fluorescence emission.[55] Because the present emission intensity of the acceptor dye is balanced between their concentration and efficiency of the "antenna effect", their emission intensity-doping concentration curve also exhibits a different trend than their single-doped counterparts.

If multiple dyes were doped in high total doping concentrations, the RET effect would be significant among the doped dyes, and the prepared multi-doped microsphere samples exhibit single excited, doping ratio-related emission signatures. Microsphere arrays with 25 fluorescence-encoded emissions have been prepared by using two dyes (Rh 110 and SRh 101) with five different concentrations each. Figure 7 a1 shows the emission spectra of a group of samples prepared with constant Rh 110 but increased SRh 101 doping concentrations. With the RET effect of the doped dyes, both dyes could be excited under the donor dye excitation (488 nm) and exhibit unique doping ratio-related emission properties. (See Figure S10 for all 25 spectra of the array). Figure 7 a2 shows the emission intensity distribution (in two channels corresponding to the doped dyes) of all five groups (25 sets) of the prepared samples. The obtained 25 sets of microspheres exhibit orderly distributed emission signatures. Microsphere arrays with 27 fluorescence-encoded emissions have been prepared by using three dyes (Acr, Flu, and Rh B) with tandem emission and excitation spectra in three different concentrations for each of the doped dye. Figure 7 b1 shows a group of the prepared samples' emission spectra (see Figure S11 for 27 spectra of the array). Figure 7 b2 shows the emission intensity distribution (in three channels corresponding to the doped dyes) of all the 27 sets of the prepared samples. All three dyes could be excited under the first donor dye (Acr) excitation and exhibit orderly distributed emission signatures related to their doping ratios. The high total doping concentration obtained by this process exhibited unique excitation and emission properties to the prepared multi-doped products with RET effects of the doped dyes. All doped dyes could be excited under single excitation, and their emission signatures are related with each other. This property could significantly facilitate fabrication of high throughput assay system. If more doping concentrations were used (e.g., 10 different doping concentrations, as used in the xMAP system provided by Luminex Corp), large encoding capacities of 100 (10 × 10) and 1000 (10 × 10 × 10) could be easily obtained.

2.7. Stability of dye-doped microspheres: investigation with dyes as self-referenced probes

Besides encoding capacity, the stabilities of the prepared fluorescence-encoded microcarriers are also significant for fabricating multiplexed high throughput assays. Fluorescent dye leakage was found in some preparations of fluorescent microspheres, which could harm the encoding information.[23] Damages of the microsphere substrate that were caused by heating or organic solvent treatment will also lead to failures in assay fabrication.

To investigate the stability of the obtained dye incorporation by the organic sol-gel process, the ANS doped MF microspheres were dispersed in water for 30 d. Given that ANS is polarity sensitive, the total fluorescent intensity of the mixture will decrease once dye molecules leak from the microspheres. Figure S12a shows the changes in fluorescence emission intensity during storage. The samples with different ANS doping concentrations showed slight changes in fluorescence emission intensities compared with those freshly dispersed counterparts. This indicates the stability of incorporation of ANS dyes.

However, most fluorescent dyes, specifically the Rhodamine dyes, are not polarity sensitive, and their incorporation stabilities could not be easily measured as ANS. A universal strategy has been developed to investigate dye incorporation stability, with the following considerations: If a couple of dyes (which could act as donor and acceptor in the RET process) were simultaneously doped into the MF microspheres, and the prepared MF microspheres were washed by centrifugation/redispersion cycles for several times, then the total doping concentration would decrease once one or both dyes leaked during the washes, resulting in changes in emission signatures, as the emission ratio of the doped dyes is related to both the total doping concentration and doping ratio. Figure S12 b shows the emission spectra of a dual-doped sample before and after 24 cycles of washes, in which the emission signature was almost unchanged even though the emission intensity decreased. The decrease in emission intensity may be ascribed to the loss of microspheres during the washes; however, the unchanged emission signature proved that no dye leakage occurred during the washes. This method was also applied for other dyes used in this study, and all of the dye incorporations are stable enough for practical applications.

The influence of autoclaving, organic solvent treatment, and mechanical stirring were also investigated. The results showed that the prepared dye-doped MF microspheres could resist heat treatment at 121 °C during the autoclaving process; the sterilized products have unchanged emission signatures. The dye-doped MF microspheres could disperse in common organic solvents, including methanol, ethanol, DMSO, and acetone, and were stable without swelling or leakage of the doped dyes. The prepared microspheres have good mechanical strength and could bear high speed stirring (4000 rpm) treatment for 6 h, without deformation or breakage. By comparison, most of the PS microspheres (similar size as counterparts) were deformed.

2.8. Preparation of multi-shell structured composite fluorescent microspheres

Given the feature and mechanism of the sol-gel process, this method not only is valid for preparing dye-incorporated monodisperse MF microspheres but also can be used to coat previously prepared particles with dye-incorporated fluorescent shells. Dye-doped MF shell layers were successfully coated onto the M@S microspheres by adding another dye and by using dye-doped M@S microspheres as seeds in a process that is similar to that of preparing dye-doped microspheres. These prepared MF@silica@MF (M@S@M) composite microspheres were then coated with a third shell layer of silica, and $(M@S)_2$ composite microspheres were prepared. Figure 8 a 1–3 show

Journal of Materials Chemistry B Accepted Manuscript

This journal is © The Royal Society of Chemistry 2012

the LSCM images of $(M@S)_2$ composite microspheres that were doped with SRh 101 and Rh 110 dyes. The prepared composite microspheres were monodisperse; both the MF core and the MF shell were evenly doped with dyes. By using blank M@S microspheres as seeds and by repeating the dye doped MF coating/silica coating processes once and twice, respectively, we prepared the $(M@S)_2$ and $(M@S)_3$ composite microspheres with different doped dyes in various MF layers. Figure 8b 1–3 show the LSCM images of $(M@S)_3$ composite microspheres that were doped with SRh 101 and Rh 110 dyes. Figure 8 b 4–6 show the 2.5D mode images of the same sample, from which the different dye-doped shells could be easily recognized. Given that MF and silica materials have different surface properties, the repeated coating also exhibited repeated altering of the zeta potentials of the prepared samples (Figure S12 c). Compared with the dual-doped MF microspheres, dyes were doped into different layers of the composite microspheres, and different doped layers were separated by silica shells. Thus, the emission signatures of these products are simply stack of the two doped dyes. Figure S12 d shows the emission spectra of the prepared composite microspheres.

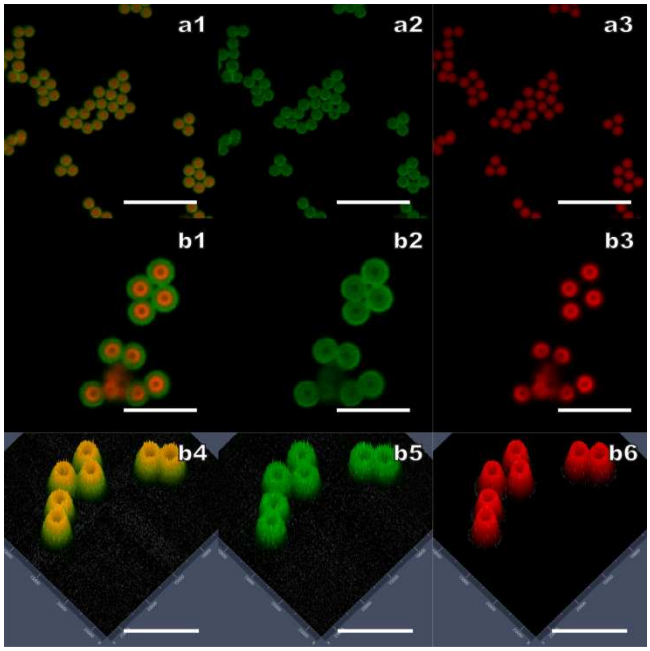

Figure 8. (a1) LSCM images of $(M@S)_2$ composite microspheres doped with SRh 101 and Rh 110 dyes. (a2-a3) Two separated channels (Rh 110 and SRh 101) of the image. (b1) LSCM image of $(M@S)_3$ composite microspheres with blank MF resin core, SRh 101 doped inner shell and Rh 110 doped out shell. The cores, inner shells and out shells are separated with silica thin layers. (b2-b3) Two separated channels (Rh 110 and SRh 101) of the image. (b4-b6) 2.5D mode images of the multi-shell structured MF microspheres, show emission intensity distribution of the microspheres. Scale bars=10 μm.

Preparation of these multi-shell structured composite microspheres demonstrated the effectiveness and agility of the organic sol-gel process. On the one hand, this method further increased the possible encoding capacity. As dyes were doped into different location of the microcarriers, the problem of spectra overlap could be partially solved, different microsphere sets could be obtained by using different dye combinations. With $(M@S)_2$ composite microspheres doped with two different dyes in the MF core and the MF shell and with 10 different dyes to choose, 45 different microspheres sets (dye combinations) could be obtained, even without considering the possible changes in doping concentrations. On the other hand, the sol-gel process provides the possibility of preparing multi-functional encoded carriers. For example, if magnetic microspheres were used as cores, fluorescence-encoded magnetic microspheres could be prepared. Related studies are in progress and will be discussed in our future reports.

3. Conclusions

In summary, an organic sol-gel process has been developed to incorporate organic dyes into the monodisperse MF microspheres. Various dyes with different physical and photoluminescence properties were incorporated into the MF microspheres during the organic sol-gel process of MF with encapsulation rates higher than 99%. The prepared products have scarcely any dye leakages after storage for one month and have demonstrated good thermal and mechanical stabilities. The dye-incorporating mechanism and RET interactions of the doped dyes have been investigated. A fluorescence-encoded microsphere array with dozens of sets was obtained by quantitatively incorporating several dyes at different doping concentrations. This novel organic sol-gel process is a promising method for the preparation of fluorescent-encoded carrier arrays with high encoding capacity and is also valid for the preparation of multi-shell structured composite fluorescent particles. These advantages indicate the wide application of this method in material and biomedical fields.

4. Experimental Section

Preparation of fluorescence-encoded MF resin microspheres:

MF resin pre-polymer solution was prepared as follows: 2.6 g of melamine was mixed with 3.7 g of paraformaldehyde and 50 mL of water. The mixture was then heated at 50 °C for 40 min with magnetic stirring (400 rpm). The obtained transparent MF pre-polymer solution was subsequently filtered with two layers of filter paper and stored at 4 °C until further use. Stock solutions of the fluorescent dyes were prepared by dissolving the dyes in DMSO at a concentration of 10 $mmol \cdot L^{-1}$. Dye-doped MF resin pre-polymer solutions of various doping concentrations were obtained by mixing a certain volume of dye stock solutions into the prepared MF resin pre-polymer solutions. In a typical preparation (for dye-doped MF resin microspheres with average diameter of 2 μm), 1 mL of dye-doped MF pre-polymer solution was mixed with 2 mL of diluted hydrochloric acid ($0.4 mmol \cdot L^{-1}$). Subsequently, the mixture was heated at 100 °C (in a boiling water bath) for 30 min to obtain a suspension of MF resin microspheres. The products were separated and washed four times with water in centrifugation/redispersion cycles before being air dried at 130 °C for 2 h in an oven. Dye encapsulation rates were obtained by comparing the dye concentration changes, which was measured by absorbance.

Preparation of core-shell and multi-shell structured composite microspheres:

Silica coating of the prepared dye doped microspheres was performed as follows: 2mL of the dye doped microspheres suspension (in water, $50 mg \cdot mL^{-1}$) was dispersed in 20 of mL ethanol, and mixed with 1.5 mL of ammonia solution, and 0.1 mL of TEOS. The mixture was incubated at 25 °C for 6 h in a swing bed. The obtained M@S core-shell microspheres were then separated and washed by centrifugation/redispersion cycles (twice with ethanol and twice with water) before drying at 130 °C for 2 h in an oven. Dye doped fluorescent MF shell

Journal of Materials Chemistry B Accepted Manuscript

coating of the as-prepared particles were performed as follows: 10 mg of M@S microspheres, 1 mL of dye-doped MF resin pre-polymer solution, and 2 mL of diluted hydrochloric acid (4 $mmol \cdot L^{-1}$) were mixed and heated at 100 °C (in a boiling water bath) for 30 min. The prepared M@S@MF composite microspheres were separated and washed four times with water in centrifugation/redispersion cycles before drying at 130 °C for 2 h in an oven.

Multi-shell structured $(M@S)_2$ and $(M@S)_3$ composite microspheres were prepared by using the prepared M@S microspheres as cores, and having MF coating/silica coating processes repeated for once and twice, respectively.

Characterization:

Scanning electron microscopy (SEM) images were obtained using a Hitachi (Tokyo, Japan) S-2700 scanning electron microscope with a 200 kV electron source. The average diameter and coefficient of variation (CV) of the microspheres were measured by counting 200 individual particles in the SEM images for each specimen.

In situ monitoring of the changes in dynamic light scattering (DLS) signals during the organic sol-gel process was conducted using a Malvern (Worcestershire, UK) Zetasizer Nano ZS90 DLS system equipped with a He–Ne laser at a wavelength of 632.8 nm. The zeta potential of the products was also measured using the same system.

LSCM images were captured using a Carl Zeiss (Oberkochen, Germany) LSM 700 laser scanning confocal microscope with 488 nm argon-ion laser excitation.

The fluorescence spectra of the samples were recorded in solutions or in suspensions by using a FluoroMax-4 fluorescence spectrophotometer (HORIBA Jobin Yvon, Kyoto, Japan). Before measuring, the dye solutions were diluted to 5 $\mu mol \cdot L^{-1}$, and the microsphere samples were prepared at a concentration of 1 $mg \cdot mL^{-1}$.

Representative fluorescence lifetimes were measured by using a time-correlated single photon counting (44MXs-B, LeCroy, USA). The samples were excited with a fiber laser (SC400-4-PP, Fianium Ltd., Southampton, UK), and the result was recorded by a single photon counting apparatus (PicoHarp300, PicoQuant, Berlin, Germany). Data were analyzed by using multiple exponential models.

Flow cytometric analyses were performed with a FACSCanto flow cytometer (BD Biosciences, San Jose, CA, USA) with 488 nm excitation. The microsphere samples were prepared at a concentration of 0.05 $mg \cdot mL^{-1}$.

Acknowledgements

This work was sponsored in part by the National Basic Research Program 973 of China (2010CB732603, 2011CB707903), National Natural Science Foundation of China (81228011, 81271686 and 61178085) and the grants of Shaanxi province science and technology and innovation project (2011KTCL03-07).

Notes and references

1. Y. Chan, J. P. Zimmer, M. Stroh, J. S. Steckel, R. K. Jain and M. G. Bawendi, *Adv. Mater.*, **2004**, 16, 2092–2097.
2. W. Wei, L. Y. Wang, L. Yuan, Q. Wei, X. D. Yang, Z. G. Su and G. H. Ma, *Adv. Funct. Mater.*, **2007**, 17, 3153-3158.
3. J. M. Behrendt, D. Nagel, E. Chundoo, L. M. Alexander, D. Dupin, A. V. Hine, M. Bradley and A. J. Sutherland, *Plos One*, **2013**, 8, DOI: 10.1371/journal.pone.0050713.
4. J. Feng, L. Xiong, S. Q. Wang, S. Y. Li, Y. Li and G. Q. Yang, *Adv. Funct. Mater.*, **2013**, 23, 340-345.
5. S. Ahn and D. R. Walt, *Anal. Chem.*, **2005**, 77, 5041-5047.
6. D. R. Walt, *Chem. Soc. Rev.*, **2010**, 39, 38-50.
7. B. Bao, F. Y. Li, H. Li, L. F. Chen, C. Q. Ye, J. M. Zhou, J. X. Wang, Y. L. Song and L. Jiang, *J. Mater. Chem. C*, **2013**, 1, 3802-3807.
8. D. Lambrechts, M. Roeffaers, G. Kerckhofs, S. J. Roberts, J. Hofkens, T. Van de Putte, H. Van Oostervvyck and J. Schrooten, *Biomaterials*, **2013**, 34, 922-929.
9. L. Cerdan, A. Costela, E. Enciso and I. Garcia-Moreno, *Adv. Funct. Mater.*, **2013**, 23, 3916-3924.
10. L. Cerdan, E. Enciso, V. Martin, J. Banuelos, I. Lopez-Arbeloa, A. Costela and I. Garcia-Moreno, *Nature Photonics*, **2012**, 6, 621-626.
11. F. Li, D. P. Josephson and A. Stein, *Angew. Chem. Int. Ed.*, **2011**, 50, 360-388.
12. M. Muller, R. Zentel, T. Maka, S. G. Romanov and C. M. S. Torres, *Chem. Mater.*, **2000**, 12, 2508-2512.
13. M. E. Leunissen, C. G. Christova, A. P. Hynninen, C. P. Royall, A. I. Campbell, A. Imhof, M. Dijkstra, R. van Roij and A. van Blaaderen, *Nature*, **2005**, 437, 235-240.
14. L. Martin-Banderas, A. Rodriguez-Gil, A. Cebolla, S. Chavez, T. Berdun-Alvarez, J. M. F. Garcia, M. Flores-Mosquera and A. M. Ganan-Calvo, *Adv. Mater.*, **2006**, 18, 559–564.
15. R. Wilson, A. R. Cossins and D. G. Spiller, *Angew. Chem. Int. Ed.*, **2006**, 45, 6104-6117.
16. S. Birtwell and H. Morgan, *Integrative Biology*, **2009**, 1, 345-362.
17. M. Y. Han, X. H. Gao, J. Z. Su and S. Nie, *Nat. Biotechnol.*, **2001**, 19, 631-635.
18. K. Braeckmans, S. C. De Smedt, M. Leblans, R. Pauwels and J. Demeester, *Nature Reviews Drug Discovery*, **2002**, 1, 447-456.
19. D. Kozak, P. Kithva, J. Bax, P. P. T. Surawski, M. J. Monteiro and M. Trau, *Chem. Commun.*, **2011**, 47, 9687-9689.
20. Q. Zhang, Y. Han, W. C. Wang, L. Zhang and J. Chang, *Eur. Polym. J.*, **2009**, 45, 550-556.
21. X. Lu, Y. Hou, J. Zha and Z. Xin, *Ind. Eng. Chem. Res.*, **2013**, 52, 5880-5886.
22. Q.-H. Liu, J. Liu, J.-C. Guo, X.-L. Yan, D.-H. Wang, L. Chen, F.-Y. Yan and L.-G. Chen, *J. Mater. Chem.*, **2009**, 19, 2018-2025.
23. Z. Zhang, Y. Long, J. Pan and X. Yan, *J. Mater. Chem.*, **2010**, 20, 1179-1185.
24. S. Qi and W. Yin, *J. Mater. Sci.*, **2011**, 46, 5288-5293.
25. T. R. Sathe, A. Agrawal and S. M. Nie, *Anal. Chem.*, **2006**, 78, 5627-5632.
26. T. Song, Q. Zhang, C. Lu, X. Gong, Q. Yang, Y. Li, J. Liu and J. Chang, *J. Mater. Chem.*, **2011**, 21, 2169-2177.
27. R. E. Gerver, R. Gomez-Sjoberg, B. C. Baxter, K. S. Thorn, P. M. Fordyce, C. A. Diaz-Botia, B. A. Helms and J. L. DeRisi, *Lab on a Chip*, **2012**, 12, 4716-4723.
28. C. Jo, H. J. Lee and M. Oh, *Adv. Mater.*, **2011**, 23, 1716-1719.
29. S. L. Wang, W. Zhao, J. Song, S. Cheng and L. J. Fan, *Macromol. Rapid. Comm.*, **2013**, 34, 102-108.

Journal of Materials Chemistry B Accepted Manuscript

This journal is © The Royal Society of Chemistry 2012

30. L. J. Wang, X. Wang, T. X. Wang, Z. J. Hu, G. Zou and Q. J. Zhang, *J. Mater. Sci.*, **2012**, 47, 2600-2606.
31. D. Nagao, N. Anzai, Y. Kobayashi, S. C. Gu and M. Konno, *J. Colloid Interf. Sci*, **2006**, 298, 232-237.
32. L. Li, C. K. Tsung, Z. Yang, G. D. Stucky, L. D. Sun, J. F. Wang and C. H. Yan, *Adv. Mater.*, **2008**, 20, 903–908.
33. W. B. Wu, M. L. Wang, Y. M. Sun, W. Huang, Y. P. Cui and C. X. Xu, *Opt. Mater.*, **2008**, 30, 1803-1809.
34. A. Schnackel, S. Hiller, U. Reibetanz and E. Donath, *Soft Matter*, **2007**, 3, 200-206.
35. X. B. Wang, G. Wang, W. W. Li, B. X. Zhao, B. Xing, Y. K. Leng, H. J. Dou, K. Sun, L. S. Shen, X. L. Yuan, J. Y. Li, K. Sun, J. S. Han, H. S. Xiao, Y. Li, P. Huang and X. Y. Chen, *Small*, **2013**, 9, 3327-3335.
36. G. Alberto, G. Caputo, G. Viscardi, S. Coluccia and G. Martra, *Chem. Mater.*, **2012**, 24, 2792-2801.
37. H. Sun, A. M. Scharff-Poulsen, H. Gu and K. Almdal, *Chem. Mater.*, **2006**, 18, 3381-3384.
38. E.-B. Cho, D. O. Volkov and I. Sokolov, *Adv. Funct. Mater.*, **2011**, 21, 3129-3135.
39. I. Sokolov, Y. Y. Kievsky and J. M. Kaszpurenko, *Small*, **2007**, 3, 419-423.
40. L. Wang and W. H. Tan, *Nano Letters*, **2006**, 6, 84-88.
41. A. Wagh, F. Jyoti, S. Mallik, S. Qian, E. Leclerc and B. Law, *Small*, **2013**, 9, 2129-2139.
42. Y. Wu, Y. Li, L. Qin, F. Yang and D. Wu, *J. Mater. Chem. B*, **2013**, 1, 204-212.
43. H. Zhou, S. Xu, H. Su, M. Wang, W. Qiao, L. Ling and D. Long, *Chem. Commun.*, **2013**, 49, 3763-3765.
44. A.-M. Caminade and C.-O. Turrin, *J. Mater. Chem. B*, **2014**, DOI: 10.1039/C1034TB00171K.
45. J. F. G. A. Jansen, E. M. M. Debrabandervandenberg and E. W. Meijer, *Science*, **1994**, 266, 1226-1229.
46. U. Maitra, S. Mukhopadhyay, A. Sarkar, P. Rao and S. S. Indi, *Angew. Chem. Int. Ed.*, **2001**, 40, 2281-2283.
47. T. Keeling-Tucker and J. D. Brennan, *Chem. Mater.*, **2001**, 13, 3331-3350.
48. B. Valeur and M. N. Berberan-Santos, *Molecular fluorescence: principles and applications*, John Wiley & Sons, Weinheim, 2013.
49. J. R. Lakowicz, *Principles of fluorescence spectroscopy*, Springer, Singapore, 2007.
50. W. M. Nau, A. Hennig and A. L. Koner, in *Springer Series on Fluorescence*, ed. O. S. Wolfbeis, Springer, Verlag Berlin Heidelberg, 2008, pp. 185-211.
51. J. Malicka, I. Gryczynski and J. R. Lakowicz, *Anal. Chem.*, **2003**, 75, 4408-4414.
52. D. Genovese, E. Rampazzo, S. Bonacchi, M. Montalti, N. Zaccheroni and L. Prodi, *Nanoscale*, **2014**, 6, 3022-3036.
53. D. Genovese, S. Bonacchi, R. Juris, M. Montalti, L. Prodi, E. Rampazzo and N. Zaccheroni, *Angew. Chem. Int. Ed.*, **2013**, 52, 5965-5968.
54. L. Marcon, C. Spriet, T. D. Meehan, B. J. Battersby, G. A. Lawrie, L. Heliot and M. Trau, *Small*, **2009**, 5, 2053-2056.
55. A. P. Demchenko, *Introduction to Fluorescence Sensing*, Springer, 2008.

Journal of Materials Chemistry B Accepted Manuscript